

# On the improvement of chimney weirs

K. Keshava Murthy and C. Rangaraj

**Abstract:** This paper is devoted to the improvement in the range of operation (linearity range) of chimney weir (consisting of a rectangular weir or vertical slot over an inward trapezium). A new and more elegant optimization procedure is developed to analyse the discharge-head relationship in the weir. It is shown that a rectangular weir placed over an inverted V-notch of depth  $0.90d$  gives the maximum operating range, where  $d$  is the overall depth of the inward trapezoidal weir (from the crest to the vertex). For all flows in the rectangular portion, the discharge is proportional to the linear power of the head,  $h$ , measured above a reference plane located at  $0.292d$  below the weir crest, in the range  $0.90d \leq h \leq 7.47d$ , within a maximum error of  $\pm 1.5\%$  from the theoretical discharge. The optimum range of operation of the newly designed weir is 200% greater than that in the chimney weir designed by Keshava Murthy and Giridhar, and is nearly 950% greater than that in the inverted V-notch. Experiments with two weirs having half crest widths of 0.10 and 0.12 m yield a constant average coefficient of discharge of 0.634 and confirm the theory. The application of the weir in the design of rectangular grit chamber outlet is emphasized, in that the datum for the linear discharge-head relationship is below the crest level of the weir.

**Key words:** weirs, notches, geometrically simple weirs, linear proportional weirs.

**Résumé :** Cet article est consacré à l'amélioration de la section opérationnelle (section linéaire) d'un déversoir en cheminée (composé d'un déversoir rectangulaire ou d'une ouverture verticale au-dessus d'un trapèze inversé). Une nouvelle procédure d'optimisation plus raffinée est développée dans le but d'analyser la relation entre le débit et la charge hydraulique dans le déversoir. Il fut montré qu'un déversoir rectangulaire placé au-dessus d'une encoche en forme de V inversé de  $0.90d$  de profondeur produit une section d'opération maximale. Pour l'écoulement dans la partie rectangulaire, le débit est proportionnel à la puissance linéaire de la charge hydraulique mesurée au-dessus du plan de référence situé à  $0.292d$  sous la crête du déversoir, pour une hauteur de charge de  $0.90d \leq h \leq 7.47d$ , avec une erreur maximale de 1.5% par rapport au débit théorique. La section opérationnelle optimale de ce déversoir nouvellement conçu est 200% plus grande que celle du déversoir en cheminée conçu par Keshava Murthy et Giridhar; et presque 950% supérieure à celle du déversoir constitué d'une encoche en forme de V inversé. Des expériences effectuées avec deux déversoirs, où  $W = 0.10$  m et  $W = 0.12$  m, appuient la théorie en produisant un coefficient de débit moyen constant de 0.634. L'utilisation du déversoir dans la conception d'une sortie d'eau rectangulaire d'un dessableur est mise en valeur. Dans cette application, la relation linéaire entre le débit et la charge hydraulique est inférieure au niveau de la crête du déversoir.

**Mots clés :** déversoir, encoche, déversoirs à géométrie simple, déversoirs proportionnels de manière linéaire.  
[Traduit par la Rédaction]

## Introduction

Thin plate weirs or sharp crested weirs are the most frequently used flow measuring devices, as they have a simple and accurate operating function (discharge-head relationship) and are inexpensive. The linear proportional weirs, which give a constant velocity in the approach channel independent of depth, have applications in diverse fields like irrigation, hydraulics, and chemical and environmental engineering and have prompted many experimental and theoretical studies (Singer and Lewis 1966; Soucek et al. 1936; Lakshmana Rao and Purushotham 1970; Lakshmana Rao and Abdul Bhukhari

1970; Keshava Murthy and Sheshagiri 1968). The exact linear weir proposed by Surto (Soucek et al. 1936) has to be designed as a compound weir consisting of a base weir and a complementary hyperbolic weir above. The complementary part of the linear weir is invariably complex and requires skilled labour for its fabrication.

Compared to the exact weirs, geometrically simple weirs consisting of quadrants of circles and straight edges are simple to cut, and still meet very well the practical requirements. These weirs give a discharge proportional to the linear power of head within a prescribed maximum error of the actual discharge within certain ranges of head.

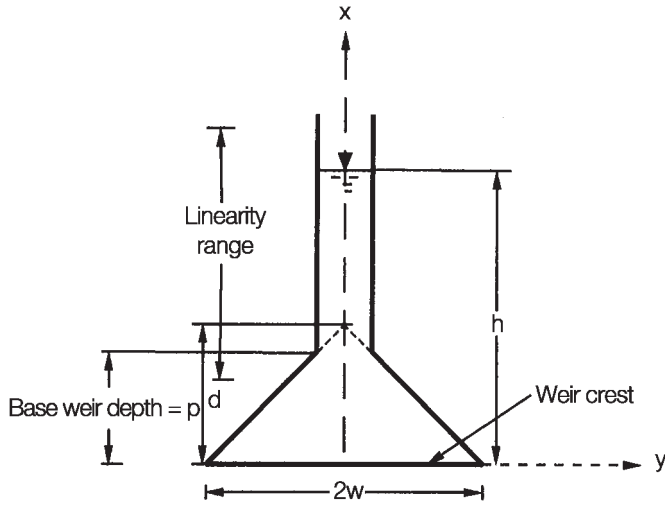
The methods of analysis adopted for chimney weirs (Keshava Murthy and Giridhar 1989), namely the methods of the tangent point and the range of points, were time consuming. A novel approach to the optimization called the oscillating point geometric method, which is outlined in this paper, is elegant and results in a drastic reduction in the computation time. This makes it possible for a detailed and extended variation of parameters in the optimization. It is entirely due to the new optimization procedure that the optimum parameters bypassed in the previous design were detected. The new range of

Received August 7, 1996.

Revised manuscript accepted January 17, 1997.

**K. Keshava Murthy and C. Rangaraj.** Department of Civil Engineering, Indian Institute of Science, Bangalore-560 012, India.

Written discussion of this article is welcomed and will be received by the Editor until December 31, 1997 (address inside front cover).

**Fig. 1.** Definition sketch of the chimney weir.

operation of the weir is 200% greater than that of the previous design. Incidentally, the range of operation (linearity range  $L_R$ ) shows an increase of 947% over that of the inverted V-notch.

The striking feature for practical engineers is that the flow taking place in the rectangular weir portion is proportional to a linear power of the head over a wide range of head. As the reference plane of the weir lies below the crest, the weir is useful as an outlet for a rectangular grit chamber.

## Formulation

The discharge,  $q$ , through the chimney weir shown in Fig. 1 is given by

$$[1a] \quad q = \frac{2}{3}C_d \sqrt{2g} 2Wh^{3/2} - \frac{8}{15}C_d \sqrt{2g} \tan \theta h^{5/2};$$

$$0 \leq h \leq p$$

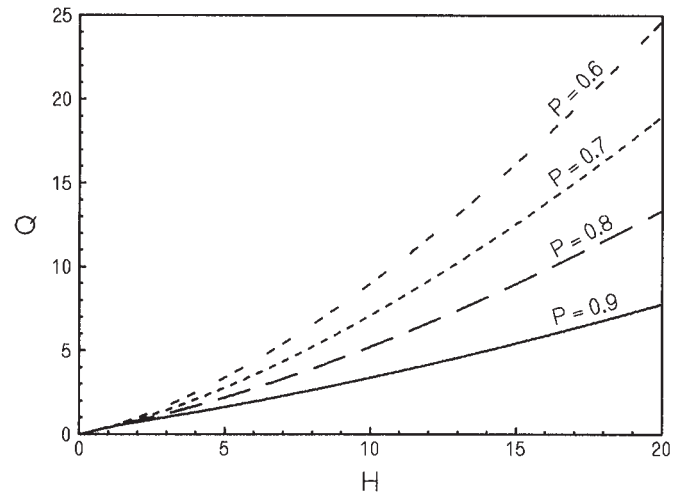
$$[1b] \quad q = \frac{2}{3}C_d \sqrt{2g} 2Wh^{3/2} - \frac{8}{15}C_d \sqrt{2g} \tan \theta \times [h^{5/2} - (h-p)^{5/2}]; \quad p \leq h \leq h_{\max}$$

where  $h$  is the head above the weir crest;  $W$  is the half crest width;  $p$  is the height of the trapezium;  $\theta$  is the side slope of the trapezium (half vertex angle of the corresponding inverted V-notch);  $g$  is the acceleration due to gravity; and  $C_d$  is the coefficient of discharge, when  $h$  is not too small (Keshava Murthy and Giridhar 1990).

The coefficient of discharge is assumed to be constant, which is generally true for sharp crested weirs and streamlined flows. The coefficient is a function of several parameters, including the head causing the flow, the dimensions of the weir in relation to the dimensions of the channel, and the crest height. The value of  $C_d$  is ascertained from experiments as in conventional weirs, and the variation of  $C_d$  will generally be within  $\pm 1\%$  of the average  $C_d$ , when  $h$  is not too small.

Equations [1a] and [1b] can be expressed, for convenience, in the nondimensional form as

$$[2a] \quad Q = \frac{2}{3}H^{3/2} - \frac{4}{15}H^{5/2}; \quad 0 \leq H \leq P$$

**Fig. 2.** Plots of  $Q$  vs.  $H$  for various values of  $P$ .

$$[2b] \quad Q = \frac{2}{3}H^{3/2} - \frac{4}{15}[H^{5/2} - (H-P)^{5/2}]; \quad H \geq P$$

where

$$Q = q / (2C_d \sqrt{2g} d^{5/2} \tan \theta)$$

$$H = h/d$$

$$P = p/d$$

and  $d$  being the overall depth of the inward trapezoidal weir.

The graph of  $Q$  vs.  $H$  is plotted in Fig. 2 for various  $P$ . It is seen to be nearly linear over a wide range of head, particularly for  $P = 0.9$ . Hence it is possible to obtain a discharge-head relationship (within the bounds of error) of the form

$$[3] \quad Q_L = mH + C$$

where  $m$  and  $C$  are the slope and the intercept of the straight line in the  $Q$  vs.  $H$  plot. It is ensured that the relative error,  $e$ , does not exceed a prefixed maximum percentage error,  $E$ , in its range of operation, i.e.,

$$[4] \quad e = \frac{|Q - Q_L|}{Q} \times 100 \leq E$$

In practice, in most discharge measurements involving weirs and notches,  $E = 2$  is normally allowed (Troskolanski 1960). Hence  $E = 1$ , adopted in this paper, is quite reasonable.

## Linear fitting

Equation [4] is used to define a permissible region within which the straight line (eq. [3]) is positioned. It follows that  $Q_L$  has to lie strictly within the permissible region bounded by

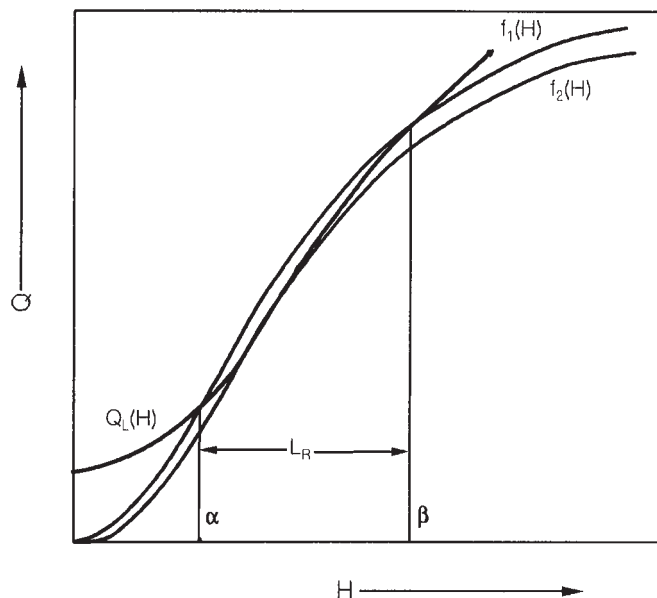
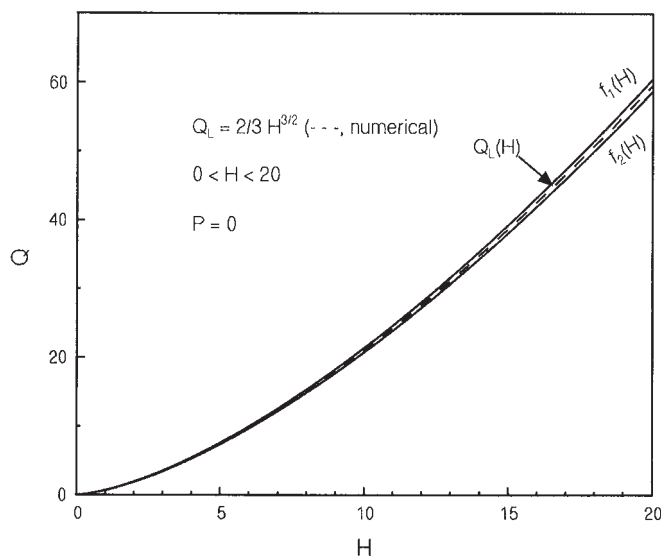
$$[5a] \quad f_1(H) = Q(H) \left( 1 + \frac{E}{100} \right)$$

$$[5b] \quad f_2(H) = Q(H) \left( 1 - \frac{E}{100} \right)$$

in its range of operation (linearity range  $L_R$ ). From Fig. 3,

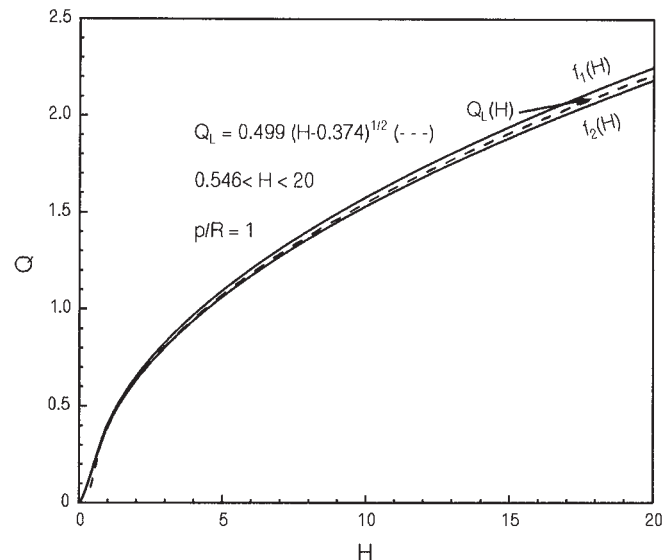
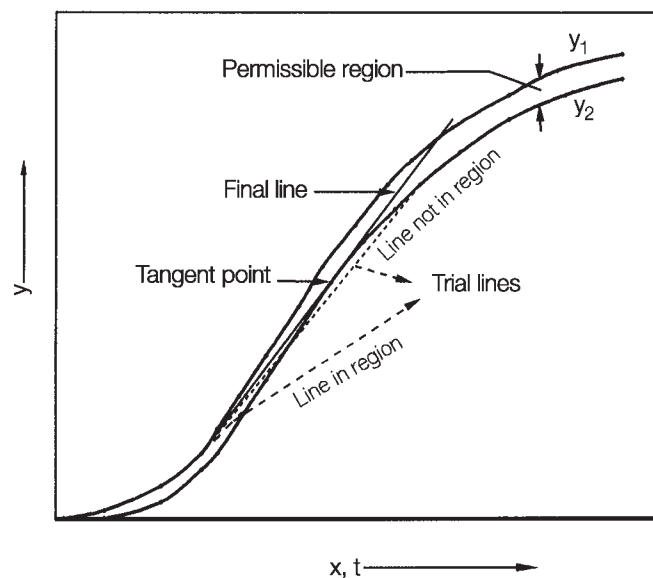
$$[5c] \quad L_R = \beta - \alpha; \quad f_2(H) \leq Q(H) \leq f_1(H)$$

The use of the boundary curves  $f_1(H)$  and  $f_2(H)$  allows the

**Fig. 3.** Sketch of the permissible region for  $Q_L$ .**Fig. 4.** Optimized value for the rectangular weir.

plotting within them of the optimum line, which acts as a visual check and allows qualitative interpretation of the results.

The optimization procedure described in the next section finds the particular straight line, within the permissible region  $f_2(H) \leq Q(H) \leq f_1(H)$ , which has a maximum horizontal projection on the head axis. That is,  $L_R$  is maximized. The linearized version of the optimization procedure described in the next section was applied for the two extreme cases,  $P = 0$  (rectangular weir) and  $P = 1$  (inverted V-notch as an orifice). The results of the optimization are shown in the discharge-head plots (Figs. 4 and 5). For the rectangular weir, the result obtained from the numerical optimization ( $q = (2/3)\sqrt{2g} (2W)h^{3/2}$ ) is the theoretical relationship. In the case of the inverted V-notch acting as an orifice, the numerical result follows very closely the theoretical discharge-head relationship. When tried upon a large variety of discharge-head curves, the proposed optimi-

**Fig. 5.** Optimization results for inverted V-notch as orifice.**Fig. 6.** Depiction of the optimization procedure.

zation procedure gave consistently precise results. It can also be applied conveniently even when the discharge-head function is not explicitly known.

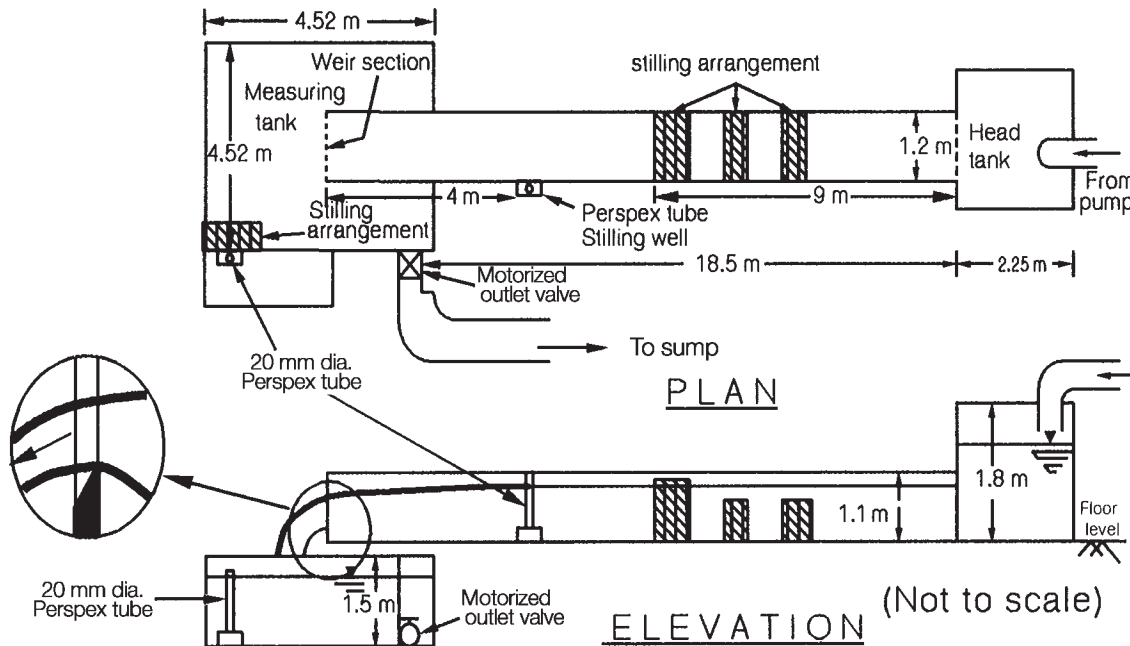
### Geometric oscillating point method

**Aim:** To find geometrically the straight line segment which is strictly inside an area bounded by a pair of curves such that its projection on the  $x$ -axis is maximum. A numerical program was developed to get the geometric solution.

Let  $y_1(x(t))$  and  $y_2(x(t))$  be the bounds of the permissible region within which the required straight line  $y_L$  is to be positioned;  $t$  takes up all integer values in  $1 \leq t \leq t_{\max}$  such that  $x(t_{\max}) = x_{\max}$  (Fig. 6). The counterparts of  $y_1(x(t))$  and  $y_2(x(t))$  in the design are  $f_1(H)$  and  $f_2(H)$ , that is,

$$y_2(x(t)) \leq y_L(x(t)) \leq y_1(x(t)); \quad 0 \leq t \leq t_{\max}$$

Line A-B is pivoted about an arbitrary point  $A(x(n), y_1(x(n)))$

**Fig. 7.** Experimental setup.**Fig. 8.** Photograph of the weir discharging.

on the top curve ( $y_1$ ), with B on the bottom curve ( $y_2$ ) and the position of B as  $B(x(m), y_2(x(m)))$ , where  $m = (k_L + k_R)/2$ ,  $k_L = n + 1$ , and  $k_R = t_{\max}$  ( $k_L < m < k_R$ ).

- Case *a*: If the line segment is entirely in the region, then any other line segment A-B\* with the position of A and B\* being  $A(x(n), y_1(x(n)))$  and  $B_*(x(m_*), y_2(x(m_*)))$ , and with its right end B\* to the left of B ( $m_* < m$ ), will have a shorter projection on the  $x$ -axis. The points on  $y_2$  between  $m_*$  and  $m$  are wiped out from consideration ( $k_L$  is moved to  $m$ ).

- Case *b*: If the entire line segment is not in the region, then any other line segment A-B\* with the position of A and B\* being  $A(x(n), y_1(x(n)))$  and  $B_*(x(m_*), y_2(x(m_*)))$ , and with its right end B\* to the right of B ( $m_* > m$ ), is also not in the region. The points on  $y_2$  between  $m_*$  and  $m$  are wiped out from consideration ( $k_R$  is moved to  $m$ ).

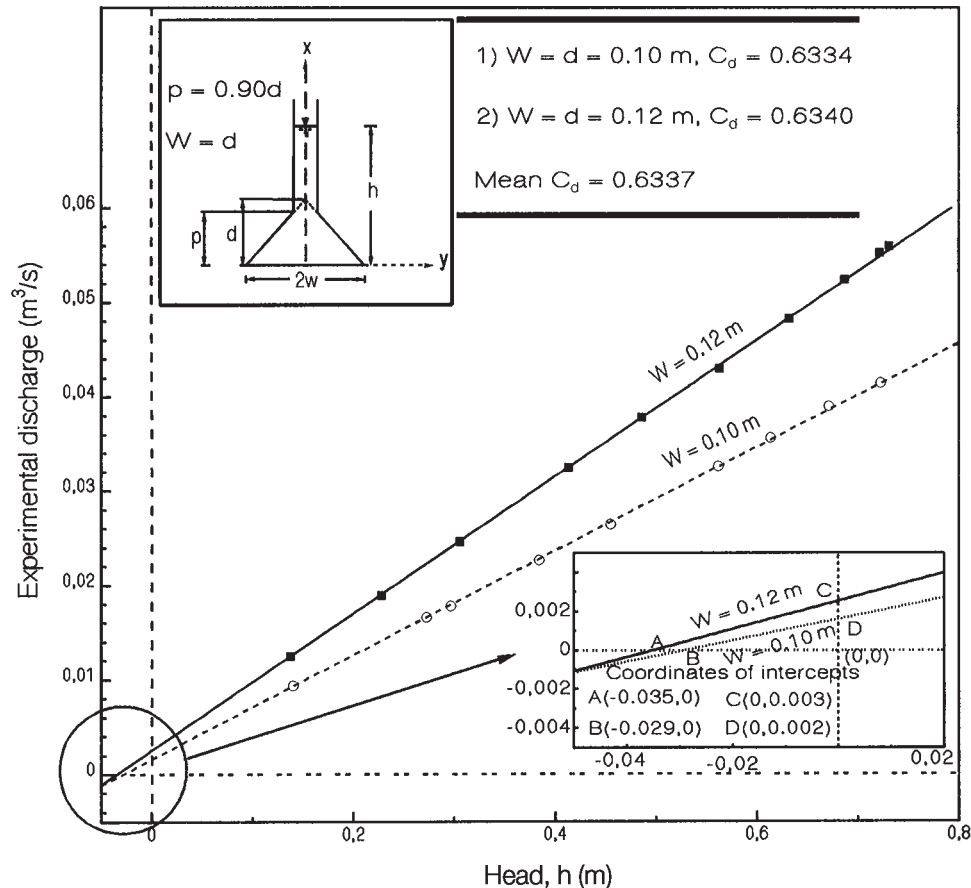
The procedure of pivoting the line about A by the algorithm given above is continued until  $k_L = k_R$  ( $k_L$  and  $k_R$  have to meet because  $k_L$  and  $k_R$  are moving in opposite directions); then the line is tangential to  $y_2$  at B. Since the line is tangential, it is extended throughout the region  $y_2(x(t)) \leq y_1(x(t)) \leq y_1(x(t))$ . The above process is repeated for all points A on  $y_1$ , and with A on  $y_2$  and B on  $y_1$ . The overall maximum linearity range and the corresponding parameters are stored.

To achieve a better simulation (obtained at a cost of a small reduction in the range of validity,  $L_R$ ), point B is chosen on the original discharge-head curve itself. When the point B is not chosen on the original discharge-head curve, the discharge equation obtained by optimization ( $q = 0.657 \sqrt{2g} (2W)h^{3/2}$ , for the limiting case,  $p = 0$  and  $n = 3/2$ ) is inaccurate.

### Estimation of the weir parameters

The optimization procedure developed is followed to obtain the optimum  $P$  for the maximum  $L_R$ . The value of the depth of the trapezium is  $0.900d$  as against the previous design value of  $0.735d$ . The discharge relation is

**Fig. 9.** Experimental discharge vs. head for  $W = 0.10$  and  $0.12$  m, with  $d = W$ ,  $p = 0.9d$ , and datum  $0.292W$  below the weir crest.



$$[6] \quad Q_L = 0.3103(H + 0.2917); \quad 0.90 \leq H \leq 7.47$$

The discharge equation of the chimney weir designed by Keshava Murthy and Giridhar (1990) is

$$[7] \quad Q_L = 0.4481(H - 0.0817); \quad 0.22 \leq H \leq 2.43$$

It is seen that although the base depth has increased to  $0.90d$  from  $0.22d$ , the linearity range increased from  $2.21d$  to  $6.57d$ , i.e., nearly by three times the old linearity range.

## Experiments

Experiments were conducted on two typical weirs with dimensions  $w = d = 0.10$  m and  $w = d = 0.12$  m. The profiles were fabricated from 6.5 mm thick mild steel sheets according to standards. The weirs had a sharp edge of 1.5 mm with a  $45^\circ$  chamfer. The weirs were fixed at the end of a rectangular channel 19.5 m long, 1.2 m wide, and 1.1 m deep with the crest set 0.20 cm above the channel bed. The channel had adequate stilling arrangements. The flow depth over the crest was measured with an electronic point gage (Fig. 7) having a least count of 0.01 mm. The experimental setup is shown in Fig. 7. Figure 8 shows the view of the weir discharging into the measuring tank.

In SI units, the head–discharge equation is

$$[8] \quad q_L = 2.7486d^{3/2} \tan \theta (h + 0.2917d); \quad 0.90d \leq h \leq 7.4697d$$

where  $q_L$  is in cubic metres per second ( $\text{m}^3/\text{s}$ ) and  $h$  in metres.

For the experimental weirs with  $W = 0.1$  and  $0.12$  m, the discharge equations are, respectively,

$$[9a] \quad q_L = 0.087C_d(h + 0.029);$$

$$0.090 \leq h \leq 0.747 \quad \text{and} \quad p = 0.090$$

$$[9b] \quad q_L = 0.114C_d(h + 0.035);$$

$$0.108 \leq h \leq 0.896 \quad \text{and} \quad p = 0.096$$

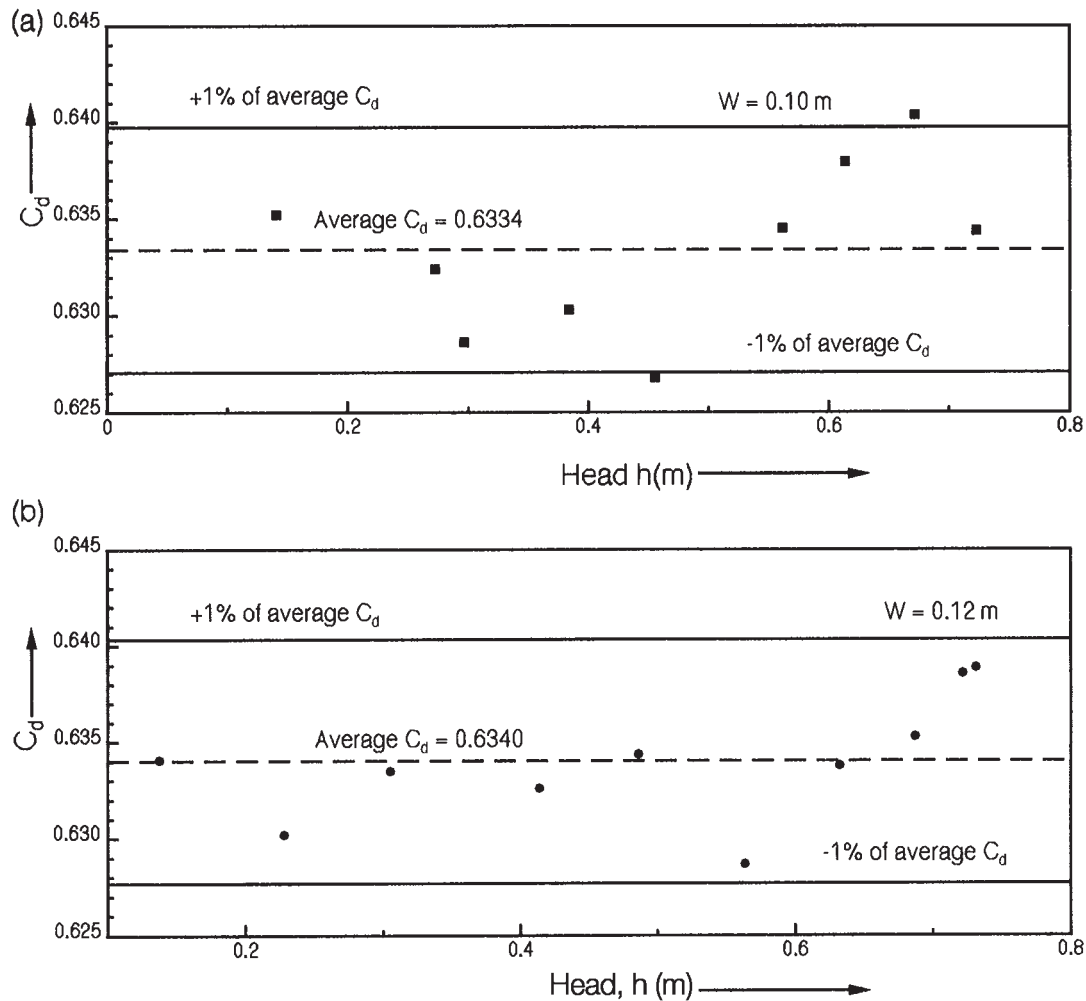
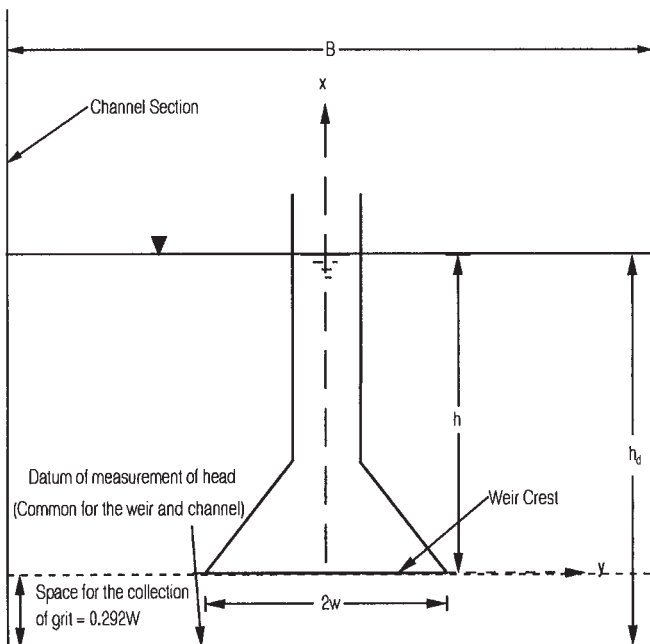
The datum lies below the crest as compared to the design of Keshava Murthy and Giridhar (1990), where it was above the crest.

Figure 9 shows the plots of the actual discharge versus head for the weirs tested. Details of the coefficient of discharge,  $C_d$ , are shown in the inset. The plots nearly coincide with the corresponding theoretical curves, which show a remarkable agreement with theory. Variation of the coefficient of discharge,  $C_d$ , with respect to the head is plotted in Fig. 10. It is seen that  $C_d$  for any head within the linearity range does not vary by more than  $\pm 1\%$  of the average  $C_d$ .

## The weir as a rectangular grit chamber outlet

Linear proportional weirs are used in the rectangular grit chamber outlet to maintain a constant average velocity in the channel for all heads.



**Fig. 10.** Variation of  $C_d$  for  $W = 0.10$  and  $0.12$  m.**Fig. 11.** The designed weir as a grit chamber outlet.

The average velocity of flow in a rectangular grit chamber is

$$[10] \quad v_{ave} \propto \frac{h + \lambda}{W_g h_d}$$

where  $\lambda$  is the datum from which the heads are measured in the weir, and  $h_d$  and  $W_g$  are the depth of flow and the width of the rectangular channel. The significance of the datum in the design of weirs was demonstrated by Keshava Murthy and Seshagiri (1968). For the velocity to be constant for all depths of flow,  $h_d$  should be equal to  $h + \lambda$ .

The Sutro weir is currently in use in rectangular grit chambers. Since the weir has to be fixed at the bed of the channel, to maintain a constant average velocity in the grit chamber, there is no gap between the crest of the weir and the bed of the channel, and sediment may get washed over. This drawback was overcome by Keshava Murthy and Seshagiri (1968) in the design of the orifice notch. In the present weir (a geometrically simple weir), it is achieved by fixing the weir crest in such a way that the reference plane of the weir coincides with the bed of the crest. This is possible because the reference plane of measurement of the head lies below the crest (see Fig. 11). The space between the crest of the weir and the bottom of the channel allows the collection of grit.

## Conclusions

This paper draws the attention to the existence of an optimum design of chimney weirs, hitherto unnoticed. The range of applicability is increased by 200%. The rectangular weir starts at  $0.9W$  in the new design, and the range of applicability of the linear relationship is entirely within it. The location of the new optimum was made possible by an elegant and swift optimization procedure. Experiments with two weirs indicate a constant average coefficient of discharge of 0.634. The results of the experiments agree very well with theory. The geometrical simplicity of the weir profile coupled with the weir's enhanced range of operation should attract the attention of practical engineers. The datum of measurement lies below the crest, which makes it possible for it to be used as a rectangular grit chamber outlet.

## Acknowledgments

The authors are grateful to the authorities of the Indian Institute of Science, Bangalore, for providing the necessary facilities for conducting this work.

## References

- Keshava Murthy, K., and Giridhar, D.P. 1989. Inverted V-notch: a practical proportional weir. *ASCE Journal of the Irrigation and Drainage Engineering Division*, **115**(6): 1035–1050.
- Keshava Murthy, K., and Giridhar, D.P. 1990. Improved inverted V-notch or chimney weir. *ASCE Journal of the Irrigation and Drainage Engineering Division*, **116**(3): 374–386.
- Keshava Murthy, K., and Giridhar, D.P. 1991. Geometrically simple linear weirs using circular quadrants: bell mouth weirs. *International Association for Hydraulic Research, Journal of Hydraulic Research*, **29**(4): 497–508.
- Keshava Murthy, K., and Gopalakrishna Pillai, K. 1978. Design of constant accuracy linear proportional weir. *ASCE Journal of the Hydraulics Division*, **104**(4): 527–541.
- Keshava Murthy, K., and Rangaraj, C. 1994. Geometrically simple exponential weir. *Hungarian Academy of Sciences, Acta Technica*, **106**(3–4): 205–221.
- Keshava Murthy, K., and Seshagiri, N. 1968. A generalized theory and experimental verification of proportional notches. *Journal of the Franklin Institute*, **285**(5): 347–363.
- Keshava Murthy, K., and Shesha Prakash, M.N. 1994. Practical constant accuracy linear weir. *ASCE, Journal of Irrigation and Drainage Engineering Division*, **120**(3): 550–562.
- Lakshmana Rao, N.S., and Abdul Bhukhari, C.H. 1971. Linear proportional weirs with trapezoidal bottoms. *International Association for Hydraulic Research, Journal of Hydraulic Research*, **9**(3): 413–427.
- Lakshmana Rao, N.S., and Purushotham, G. 1970. Experimental studies on linear proportional Weirs with triangular bottoms. *International Association for Hydraulic Research, Journal of Hydraulic Research*, **8**(4): 449–455.
- Singer, J., and Lewis, D.C.G. 1966. Proportional flow for automatic sampling or dosing. *Water and Water Engineering*, **70**(841): 105–111.
- Soucek, E., Howe, H.E., and Mavis, F.T. 1936. Suro weir investigations furnish discharge coefficients. *Engineering News Record*, **127**: 679.
- Troskolanski, A.T. 1960. *Hydrometry: Theory and practice of hydraulic measurements*, Pergamon Press, New York, pp. 301–302.

## List of symbols

- A left end of the line segment  
 B right end of the line segment  
 B\* right end of the line segment when it is shifted from B with A held fixed  
 C constant in the relationship  $Q_L = mH + C$   
 $C_d$  coefficient of discharge  
 $d$  overall depth of the inward trapezoidal weir (from the crest to the vertex)  
 $e$  deviation of  $Q_L$  from the theoretical discharge  $Q$   
 $E$  prefixed maximum permissible percentage error in discharge computations; 1.5% for the present design  
 $f_1(H)$  upper bound for the linear  $H$ – $Q$  function to lie within  
 $f_2(H)$  lower bound for the linear  $H$ – $Q$  function to lie within  
 $h$  depth of flow above the weir crest  
 $h_d$  depth of flow in the channel  
 $H$  nondimensional head ( $H = h/d$ )  
 $K$   $2C_d \sqrt{2g}$   
 $L_R$  linearity range  
 $m$  proportionality constant in the linear head–discharge relationship  
 $n$  particular value of  $t$   
 $p$  depth of the inward trapezoidal weir at which the rectangular weir is fitted  
 $P$   $p/d$   
 $q$  discharge through the weir  
 $Q$  total nondimensional discharge through the weir ( $Q = q/(K \tan \theta d^{5/2})$ )  
 $Q_L$  nondimensional head–discharge function  
 $t$  a parameter taking integer values  
 $v_{ave}$  average velocity in the rectangular channel  
 $W$  half crest width of the weir  
 $y_1(x)$  upper bound of the permissible region  
 $y_2(x)$  lower bound of the permissible region  
 $\alpha$  base flow depth or the starting point of the linearity range  
 $\beta$  terminal point of the linearity range  
 $\lambda$  datum constant  
 $\theta$  side slope of the trapezium (half vertex angle of the corresponding inverted V-notch)